

Two Special Finite Elements for Modelling Rolling Contact in a Multibody Environment

A. L. Schwab and J. P. Meijaard

Laboratory for Engineering Mechanics
Delft University of Technology
Mekelweg 2, NL-2628 CD Delft, The Netherlands
Phone: +31-15-2782701, Fax: +31-15-2782150
Email: a.l.schwab@wbmt.tudelft.nl

Keywords: Flexible Multibodies, Vehicle Dynamics, Wheel-Rail Contact.

Abstract

In this paper we describe two special finite element types for the modelling of rolling contact. The first element is a disk bounded by a sharp edge which can roll over a smooth three-dimensional surface. This element models the rolling contact phenomena of pneumatic tires that support road vehicles. The second finite element describes the kinematic contact between two arbitrary three-dimensional bodies with smooth bounded surfaces. In particular the higher kinematic pair of a wheel and rail as can be found in railway vehicles is analysed. Both element types are incorporated in a general multibody dynamics software package that handles the modelling of the other rigid or flexible bodies in the system and their interconnections. The disk element is illustrated in the stability analysis of the rectilinear motion of a rolling disk. Two tests on a single wheelset moving on a tangent track illustrate the use of the wheel-rail contact element.

1 Introduction

In the dynamic analysis of flexible multibody systems the finite element method has proved a successful instrument [1]. For the analysis of road and track-guided vehicles this success depends upon a suitable finite element type for the description of the geometry of the rolling contact.

In our approach the three coordinates of the contact point are introduced as an extra node. The geometric conditions of contact are that this node is on both contacting surfaces and the normals are collinear. The advantage of this formulation over the descrip-

tion by curvilinear coordinates as used by several other investigators [2; 3; 4] is that the number of coordinates, and also the number of constraints, is reduced by one and the contact point becomes an ordinary node in the finite element formulation. The longitudinal slip, the side slip and the spin are defined in terms of deformation rates. Pure rolling can be established by imposing zero slip constraints, which are non-holonomic, on the system. Whereas in the case of slip a contact force model, the constitutive behaviour, can be added either in the form of empirical or semi-empirical functions or tabulated data. The creep forces usually depend on the slip quantities and the normal force. In the wheel-rail contact the bodies are stiff and the normal deformation is usually neglected. The normal force now becomes a reaction force that depends on the accelerations in the system. Owing to the non-linearity of the creep force laws, the accelerations have to be determined in an iterative way for a given state of motion. However, if the normal compliance of the rails is considered the normal force can directly be obtained from the constitutive relation.

For a wheelset which moves along a central line on the track most displacement components have only small deviations from their nominal values and hence partially linearized equations of motion can be applied. However, the non-linearity of the geometric contact and the creep laws have to be retained. The case of double point contact, that is, contact between a wheel and a rail not only occurs at a point on the wheel tread, but may also occur at a point on the wheel flange, can easily be handled by introducing an additional contact pair that becomes active at the moment that the flange hits the rail. In order to avoid the necessity to solve impact equations with the possible result of unrealistic lift-off of wheels, the compliance of rail and flange is included.

2 Three-Dimensional Wheel

The three-dimensional flexible wheel element is a model of a disk bounded by a sharp edge with radius r , which can roll over a fixed surface. The position and orientation of the wheel will be described by the position of the wheel centre \mathbf{w} , the orientation of the wheel axle \mathbf{e}_w , specified by the four Euler parameters $q = (q_0, \mathbf{q})$, which correspond to a rotation matrix \mathbf{R} , and the position of the contact point \mathbf{c} as shown in Figure 1. Note that

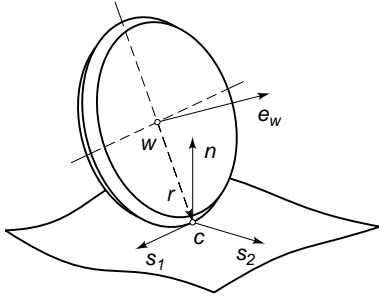


Figure 1. Three-dimensional wheel element

the contact point is a geometric point, it is not a fixed material point of the wheel nor of the surface. In the case of pure rolling as a rigid body the element has three degrees of freedom, while we have ten coordinates describing the position and orientation. Hence we have to impose seven constraints upon the velocities. Only two of these constraints are non-holonomic constraints, all other velocity constraints are time derivatives of holonomic conditions originating from the rigidity conditions.

The first two generalized strains for the wheel element are defined as

$$\begin{aligned}\varepsilon_1 &= \frac{1}{2}(\mathbf{r} \cdot \mathbf{r} - r_0^2)/r_0 \\ \varepsilon_2 &= \mathbf{e}_w \cdot \mathbf{r}\end{aligned}\quad (1)$$

with the radius vector $\mathbf{r} = \mathbf{c} - \mathbf{w}$, the undeformed radius length r_0 and the rotated wheel axle $\mathbf{e}_w = \mathbf{R}\mathbf{e}_w$. The first strain, ε_1 , is a quadratic approximation of the elongation of the wheel radius. Using this approximation has the advantage of constant second order derivatives. The second strain is a measure for the lateral bending deformation. The next two generalized strains deal with the surface contact,

$$\begin{aligned}\varepsilon_3 &= g(\mathbf{c}) \\ \varepsilon_4 &= (\mathbf{r} \times \mathbf{e}_w) \cdot \mathbf{n}\end{aligned}\quad (2)$$

with the surface defined by a function $g(\mathbf{c}) = 0$. The normal vector to the surface in the contact point is given by $\mathbf{n} = \nabla g(\mathbf{c})$.

Note that this is not a unit vector. Normalization of this vector would lead to far more complex first and higher order partial derivatives of ε_4 . The third strain is a measure for the distance of the contact point with respect to the surface. By imposing the constraint $\varepsilon_3 = 0$ the contact point will stay on the surface. By setting the fourth strain to zero we are certain of having only one contact point or in other words, the rim must be tangent to the surface. The last strain is used for the normalization condition, $|q| = 1$, which we have to impose on the four Euler parameters $q = (q_0, \mathbf{q})$ to ensure that they represent a three-dimensional finite rotation, and reads

$$\varepsilon_q = q_0^2 + \mathbf{q} \cdot \mathbf{q} - 1. \quad (3)$$

The constraint, $\varepsilon_q = 0$, is not part of the wheel element but comes with every set of Euler parameters and is shown here for completeness.

Finally we define the longitudinal and lateral slip. The velocity of the material point of the wheel at contact in \mathbf{c} is given by $\mathbf{v} = \dot{\mathbf{w}} + \boldsymbol{\omega} \times \mathbf{r} + \mathbf{v}_\varepsilon$. In this expression \mathbf{v}_ε stands for the contribution to the velocity due to the rate of deformation of the wheel, and $\boldsymbol{\omega}$ is the angular velocity of the wheel. In the contact point the two orthogonal surface tangents are the longitudinal direction $\mathbf{r} \times \mathbf{e}_w$ and the lateral one $\mathbf{n} \times (\mathbf{r} \times \mathbf{e}_w)$. With these directions the longitudinal and lateral slip are defined as

$$\begin{aligned}s_1 &= (\mathbf{r} \times \mathbf{e}_w) \cdot (\dot{\mathbf{w}} + \boldsymbol{\omega} \times \mathbf{r}) \\ s_2 &= (\mathbf{n} \times (\mathbf{r} \times \mathbf{e}_w)) \cdot \dot{\mathbf{c}}\end{aligned}\quad (4)$$

Since \mathbf{v}_ε is perpendicular to the longitudinal direction it is not included in the definition of s_1 . If the generalized coordinates which describe the positions and orientation of the element are grouped together in a vector $\mathbf{x}^T = (\mathbf{w}^T, \mathbf{c}^T, q_0, \mathbf{q}^T)$, and the vector of slips is denoted by \mathbf{s} , the expressions for the slip can be written symbolically as

$$\mathbf{s} = \mathbf{V}(\mathbf{x})\dot{\mathbf{x}}. \quad (5)$$

Pure rolling is described by zero slips, $\mathbf{s} = \mathbf{0}$.

With the vector of element strains expressed as $\boldsymbol{\varepsilon} = \mathbf{D}(\mathbf{x})$, the generalized stresses $\boldsymbol{\sigma}$ and forces $\boldsymbol{\lambda}$ dual to the slips can be interpreted from the element equilibrium equation,

$$\mathbf{f} = \mathbf{D}_{,\mathbf{x}}^T \boldsymbol{\sigma} + \mathbf{V}^T \boldsymbol{\lambda}. \quad (6)$$

The first two generalized stresses σ_1 and σ_2 are the radial force and the lateral bending force. The third stress, σ_3 is the force in the contact point exerted on the wheel perpendicular to the

surface. The fourth stress, dual to the tangent condition $\varepsilon_4 = 0$, can be interpreted as a torque divided by the radius of the wheel acting in the contact point along the s_2 direction. This torque is always zero under normal loading. Only when forces are applied in the contact point \mathbf{c} , which is unrealistic since this node is a non-material point, the torque will be non-zero. The generalized forces dual to the slip can be interpreted as λ_1 being the longitudinal contact force divided by the actual radius length $|\mathbf{r}|$ and λ_2 the lateral force divided by the actual radius and normal vector length $|\mathbf{r}||\mathbf{n}|$. This scaling seems awkward but excluding normalization in the slip definitions (4) results in much simpler first and higher order partial derivatives.

Each individual strain can be assumed either zero or non-zero, representing respectively the rigid and the deformable case. In the deformable case a constitutive equation relating σ to ε has to be applied. The same holds for a longitudinally and/or laterally slipping wheel. In this case the generalized stresses, in particular the normal stress σ_3 , are usually incorporated in the constitutive behaviour, taking the form $\lambda = \lambda(\mathbf{s}, \sigma)$. A detailed description of the constitutive behaviour of three-dimensional elastic bodies in rolling contact can be found in the books by Kalker [5] and Johnson [6].

3 Wheel-Rail Contact Element

A special finite element that describes the contact between two bodies, of which one can move in space, henceforth called the wheel, and the other is fixed to the ground, henceforth called the rail, is described as follows. The nodal coordinates are the po-

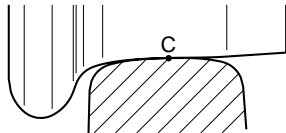


Figure 2. Wheel-rail contact pair with contact point C.

sition coordinates of the centre of the wheel, $\mathbf{w} = (w_x, w_y, w_z)^T$, the four Euler parameters that describe the rotation of the wheel with respect to a nominal position, $q = (q_0, \mathbf{q})$, which correspond to a rotation matrix \mathbf{R} , and the coordinates of the contact point, $\mathbf{c} = (c_x, c_y, c_z)^T$. Four holonomic generalized deformations are defined, which, if required to be zero, give the contact conditions, as

$$\begin{aligned} \varepsilon_1 &= g_w(\bar{\mathbf{r}}) = g_w(\mathbf{E}^{0T} \mathbf{R}^T (\mathbf{c} - \mathbf{w})), \\ \varepsilon_2 &= g_r(\mathbf{c}), \\ \varepsilon_3 &= \mathbf{n}_w \cdot \mathbf{a}_r = (\mathbf{R} \mathbf{E}^0 \bar{\nabla} g_w) \cdot \mathbf{a}_r, \\ \varepsilon_4 &= \mathbf{n}_w \cdot \mathbf{b}_r = (\mathbf{R} \mathbf{E}^0 \bar{\nabla} g_w) \cdot \mathbf{b}_r. \end{aligned} \quad (7)$$

Here, $\bar{\mathbf{r}}$ are the coordinates of the contact point of the wheel expressed in a body-fixed frame, \mathbf{E}^0 is the orientation of the wheel in the reference position, the functions g_w and g_r yield a measure of the outward distance to the surfaces of the wheel and rail respectively, \mathbf{n}_w is the normal to the surface of the wheel, and \mathbf{a}_r and \mathbf{b}_r are two tangent vectors to the surface of the rail in the direction of the track and in a perpendicular direction. The operator $\bar{\nabla}$ denotes differentiation with respect to the body-fixed coordinates $\bar{\mathbf{r}}$. The first two deformations measure the distance to the bounding surfaces, which may be unequal to zero if separation or indentation is possible. The third and fourth deformation are always zero, because they define the contact point or potential contact point.

In addition to these four deformations, three non-holonomic slip functions are defined as

$$\begin{aligned} s_1 &= \mathbf{v}_c \cdot \mathbf{a}_r, \\ s_2 &= \mathbf{v}_c \cdot \mathbf{b}_r, \\ s_3 &= \boldsymbol{\omega}_w \cdot \mathbf{n}_r, \end{aligned} \quad (8)$$

where $\mathbf{v}_c = \dot{\mathbf{w}} + \boldsymbol{\omega}_w \times (\mathbf{c} - \mathbf{w})$ is the velocity of the material point of the wheel at the contact point, \mathbf{n}_r is a normal vector to the rail at the contact point, and $\boldsymbol{\omega}_w$ is the angular velocity of the wheel. The slips s_1 and s_2 are the slip velocities in the two tangent directions and s_3 is the spin. Pure rolling can be modelled by making the slip velocities zero.

The generalized stresses dual to the generalized deformations are obtained either as constraint forces or are given by constitutive relations, the creep laws. The creep forces depend on the position of the contact point, the rolling velocity, here defined as $\|\dot{\mathbf{c}} - \mathbf{v}_c/2\|$, the normal force at the contact point and the slips (8). If the constitutive relations depend on the normal force that is a constraint force, the accelerations have to be determined in an iterative way, as in the case of dry friction.

4 Rolling Disk Example

One of the simplest and most intriguing examples of a spatial non-holonomic system is a disk rolling without slip on a horizontal plane. From experience we know that such an object, if given enough initial speed, shows stable motion which is quite different from the behaviour at low speed. We will investigate the stability of the rectilinear motion with the help of the wheel element from Section 2. The rolling of a disk on a horizontal plane has been studied in detail by for example Neĭmark and Fufaev [7] and we shall compare the results. The finite element model of the system consists of a wheel element, rolling on a horizontal plane $z = 0$, and three orthogonal hinges attached to the wheel centre to describe the three degrees of freedom: pitch, roll and yaw (Figure 3). The two kinematic coordinates are the x and y position of the point of contact in the plane. We will assume that the infinitesimally thin disk has uniformly distributed

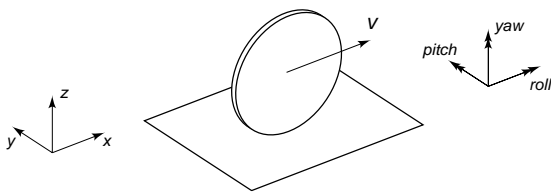


Figure 3. Disk rolling on a horizontal plane.

unit mass m , unit radius r and a unit gravitational force field g in the downward direction.

The stability of the rectilinear motion at longitudinal speed v is investigated by the determination of the eigenvalues of the linearized equations of motion. The method for deriving these equations in a systematic manner can be found in [8]. The dimension of the eigenvalue problem is eight; namely two times the number of degrees of freedom plus the number of kinematic coordinates. Beforehand we know that there are six zero eigenvalues. The first two pairs are a consequence of the two cyclic coordinates, the pitch and the yaw, in the system. The potential energy is only a function of the rotation along the longitudinal axis, the roll angle. The last two zero eigenvalues describe the kinematic motion of the point of contact (x, y) . The remaining two non-zero eigenvalues of the perturbed rectilinear motion in the speed range of $0 \leq v \leq 1$, where speed scales according to \sqrt{gr} , are shown in Figure 4. At low speeds there are two equal and opposite real

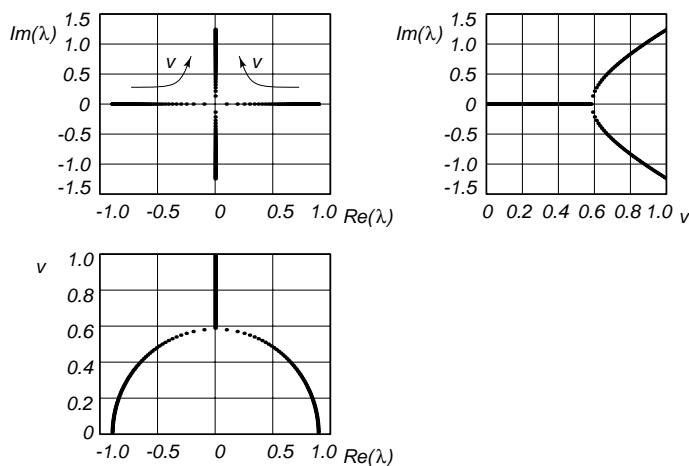


Figure 4. Root loci of the eigenvalues λ for the rectilinear motion of a rolling disk on a horizontal plane in the speed range of $0 \leq v \leq 1$.

eigenvalues describing unstable perturbed motion, just like an inverted pendulum. At increasing speed these eigenvalues move to zero, where at the critical speed [7], $v = 1/\sqrt{3} \approx 0.58$, they

change into a pair of conjugated imaginary values which describe an undamped oscillatory motion. The corresponding eigenmode is of the slalom type and can best be characterised by a 90° phase angle between the roll and the yaw motion. Further increase of the speed shows an approximately linear increase in the eigenvalues.

The unstable perturbed motion, below the critical speed, is illustrated by a transient analysis. The initial conditions are a vertical position with a forward speed of $v = 0.4116$, an angular roll velocity of -0.01 and a zero yaw rate. The path of the centre of the disk and the path of the contact point in the plane are shown in Figure 5 for the time period of 87 units, where one time unit scales according to $\sqrt{r/g}$. The low roll velocity starts

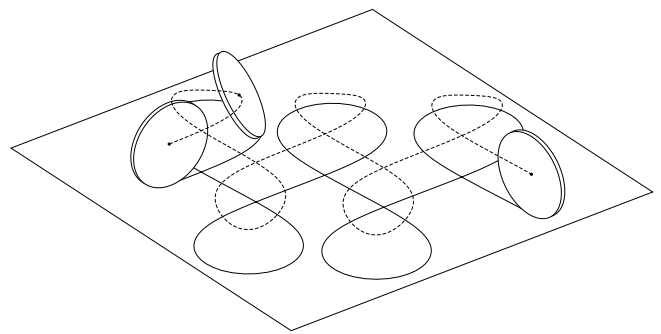


Figure 5. Path of a rolling disk on a horizontal plane at subcritical speed for a time period of 87 units, with an initial forward velocity 0.4116 and a roll velocity -0.01 .

the initially exponentially increasing inclination of the disk, after which it makes a sharp turn and rises up again to the vertical position. This motion is repeated at equal time intervals and in alternating turning directions. The unstable rectilinear motion is transformed into a quasiperiodic motion where the disk continues to wobble forward.

The forces in the contact point exerted by the wheel on the plane for this quasiperiodic motion are shown in Figure 6. During cornering the lateral and normal force increase in magnitude whereas the longitudinal contact force shows a short oscillation indicating an accelerating and decelerating longitudinal motion. The ratio of the in-plane contact force to the normal contact force during cornering is at most 0.52. The friction coefficient must be above this value to ensure rolling without slipping.

However, if we assume a force contact model which is linear in the slip velocities at the contact point then the disk on a smooth surface will slip into an almost cyclic motion during the first turn. In this motion the centre of mass mainly moves in the downward direction while the rotation of the point of contact increases rapidly. The disk eventually will come to the singular horizontal rest position in a finite time. Compare this with the

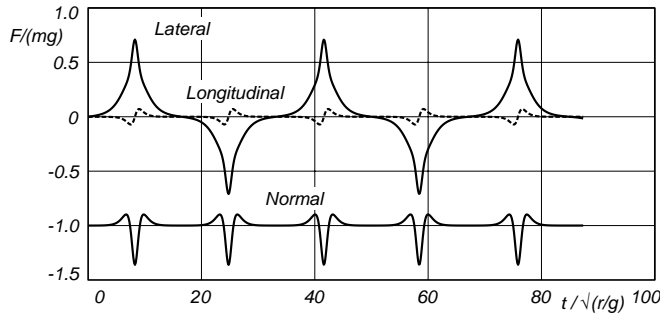


Figure 6. Forces in the contact point of a rolling disk on a horizontal plane at subcritical speed for a time period of 87 units, with an initial forward velocity 0.4116 and a roll velocity -0.01.

behaviour of the contemporary executive toy known as “Euler’s disk”; a smooth edged disk on a slight concave supporting bowl which whirrs and shudders to a horizontal rest [9].

5 Wheelset Example

The use of the wheel-rail element is illustrated in two test examples which involve a single wheelset on a tangent track that is suspended in a moving frame that imposes a constant forward velocity on the centre of the wheelset. The chosen profiles are S1002 for the wheel bands and UIC60 for the rails, as given in [10]. The track width of the wheelset is 1.5 m and the gauge between the rails is 1.435 m, with slant 1/40 or 1/20.

5.1 Klingel Motion of a Wheelset

The first test involves the kinematic, or Klingel, motion of the wheelset. The slip velocities are put equal to zero in this case. Because the system becomes overconstrained, axial deformation of the axle of the wheelset is allowed. The theoretical wave length λ for small amplitudes for this motion is

$$\lambda = 2\pi \sqrt{\frac{br_0}{\gamma} \frac{(\rho_w - \rho_r)}{\rho_w} \frac{b}{(b + \rho_r \sin \alpha)}}, \quad (9)$$

where $\gamma = \tan \alpha$ is the conicity, b is half the distance between the two contact points, r_0 is the rolling radius, ρ_r is the radius of curvature of the rail (convex positive), and ρ_w is the radius of curvature of the wheel in the meridional plane (concave positive). For the rail slant 1/40, $\lambda = 14.463$ m, and for the rail slant 1/20, $\lambda = 39.589$ m, which agree well with numerically obtained results. For larger amplitudes, the wave lengths decrease.

5.2 Critical Speed of Wheelset

As a second test example, the critical speeds are determined. The mass of the wheelset is 1887 kg, its principal moments of in-

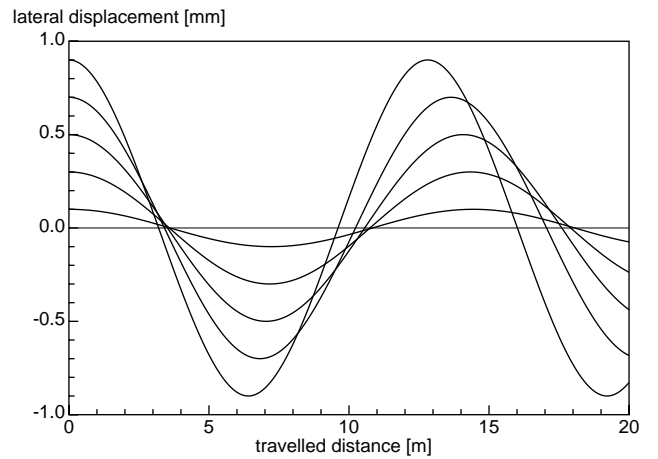


Figure 7. Kinematic motion with various amplitudes; rail slant 1/40.

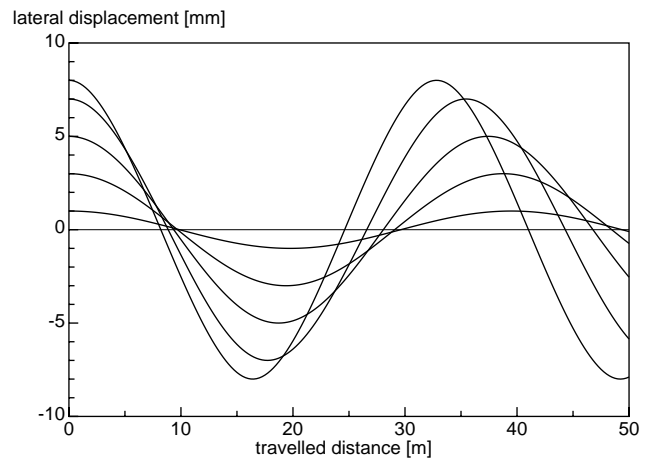


Figure 8. Kinematic motion with various amplitudes; rail slant 1/20.

ertia are 1000, 100, and 1000 kgm^2 , and the total vertical load is 173 226 N. The linear creep coefficients are 12 MN in both directions and 20 kNm as a coupling between spin and lateral creep. The effect of saturation is included according to the formula of Vermeulen and Johnson [11]. At a rail slant of 1/40, the critical speed is $V_{cr} = 30.4$ m/s without spring supports and $V_{cr} = 55.5$ m/s with a yaw spring of stiffness 816 kNm/rad. The stability of the free wheelset at low speeds is caused by the positive gravitational stiffness. For a rail slant of 1/20, the free wheelset is unstable at low speeds, because the gravitational stiffness is negative. With a yaw spring with stiffness 816 kNm/rad, the critical speed is $V_{cr} = 130.0$ m/s.

At the critical speeds, subcritical Hopf bifurcations occur. This can be understood, because the Klingel wavelength decreases with increasing amplitude. For speeds above the critical speed, limit cycle motion with flange contact is found.

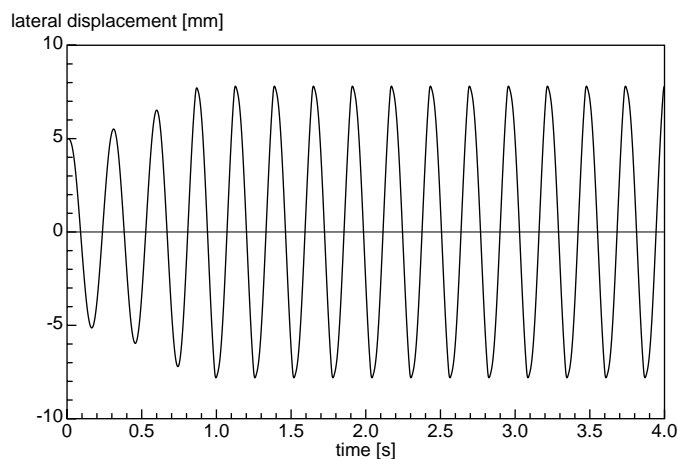


Figure 9. Limit cycle motion at $V=131$ m/s; rail slant $1/20$; yaw stiffness 816 kNm/rad.

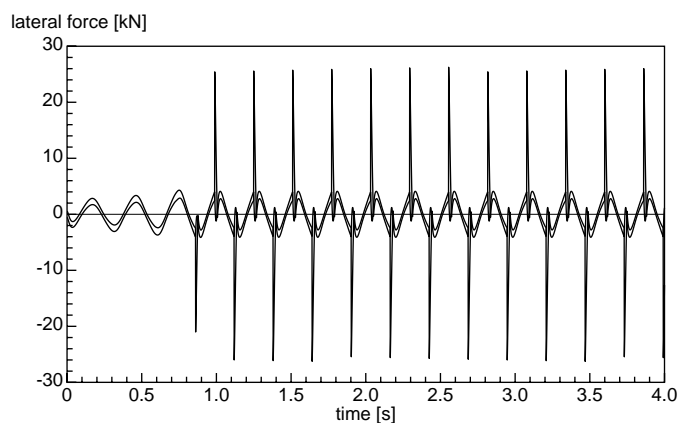


Figure 10. Lateral forces at limit cycle motion at $V=131$ m/s; rail slant $1/20$; yaw stiffness 816 kNm/rad.

6 Conclusion

It has been shown that, in principle, the proposed contact elements can be used to model the dynamic behaviour of road and railway vehicle systems. The elements have the advantage that they fit into an existing framework for modelling multibody systems and that they use a smaller number of constraint equations than some other formulations. The wheel-rail contact element shares the disadvantage with many other formulations that it is difficult to take into account the possible occurrence of double point contact, especially if both contact points are located at closely spaced points on the wheel tread. In addition, the jumps in curvature of the unworn profiles cause jumps in forces and in the speed of the contact point. A further investigation in a proper modelling of the contact seems to be worth while.

References

- [1] Jonker, J. B., and Meijaard, J. P., "SPACAR—computer program for dynamic analysis of flexible spatial mechanisms and manipulators," in Schiehlen, W. (ed.), *Multibody Systems Handbook*, Springer-Verlag, Berlin, 1990, pp. 123–143.
- [2] Fisette, P., and Samin, J. C., "A new wheel/rail contact model for independent wheels," *Archive of Applied Mechanics*, **64** (1994), pp. 180–191.
- [3] Glocker, C., "Formulation of spatial contact situations in rigid multibody systems," *Computer Methods in Applied Mechanics and Engineering*, **177** (1999), pp. 199–214.
- [4] Shabana, A. A., and Sany, J. R., "An augmented formulation for mechanical systems with non-generalized coordinates: application to rigid body contact problems," *Nonlinear Dynamics*, **24** (2001), pp. 183–204.
- [5] Kalker, J. J., *Three-Dimensional Elastic Bodies in Rolling Contact*, Kluwer, Dordrecht, 1990.
- [6] Johnson, K. L., *Contact Mechanics*, Cambridge University Press, Cambridge, UK, 1985.
- [7] Neĭmark, Ju. I., and Fufaev, N. A., *Dynamics of Nonholonomic Systems*, (Translated from the Russian edition, Nauka, Moscow, 1967), A.M.S., Providence RI, 1972.
- [8] Schwab, A. L., and Meijaard, J. P., "Dynamics of flexible multibody systems having rolling contact: Application of the wheel element to the dynamics of road vehicles," *Vehicle System Dynamics Supplement* **33** (1999), pp. 338–349.
- [9] Moffatt, H. K., "Euler's disk and its finite-time singularity," *Nature* **404** (2000), pp. 833–834.
- [10] Kortüm, W., and Sharp, R. S. (eds), "Multibody Computer Codes in Vehicle System Dynamics," *Vehicle System Dynamics Supplement*, **22** (1993).
- [11] Vermeulen, P. J., and Johnson, K. L., "Contact of nonspherical elastic bodies transmitting tangential forces," *ASME Journal of Applied Mechanics*, **31** (1964), pp. 338–340.